High-resolution core-level study of 6*H*-SiC(0001)

L. I. Johansson, Fredrik Owman, and Per Mårtensson
Department of Physics, Linköping University, S-58183 Linköping, Sweden
(Received 26 October 1995)

A photoemission investigation using synchrotron radiation of the (0001) surface of 6*H*-SiC is reported. The studies were concentrated on the $\sqrt{3}\times\sqrt{3}$-*R*30° and $6\sqrt{3}\times6\sqrt{3}$-*R*30° reconstructed surfaces, but results from the chemically prepared unreconstructed 1×1 surface are also presented. Core-level and valence-band spectra recorded from the 1×1 surface show strong oxygen derived features. For the $\sqrt{3}$ and $6\sqrt{3}$ reconstructed surfaces, which were prepared by heating the 1×1 surface to temperatures of ca. 950 °C and 1150 °C, respectively, no oxygen derived features are detected. The core-level and valence-band spectra are found to be significantly different on these reconstructed surfaces. Recorded high-resolution core-level spectra reveal unambiguously the presence of surface shifted components in both the Si 2*p* and C 1*s* core levels on the reconstructed surfaces. For the $\sqrt{3}$ reconstruction, two surface shifted components are observed both in the Si 2*p* and C 1*s* level. These findings cannot be explained by a structural model composed of Si or C adatoms on top of a Si-C bilayer. For the $6\sqrt{3}$ reconstruction, the surface region is found to contain a considerably larger amount of carbon. This carbon is found not to be graphitic, since surface shifted C 1*s* components with binding energies different from the graphitic C 1*s* peak are observed. Clear evidence of graphitization is revealed only after heating to a higher temperature than that required for observing a well-developed $6\sqrt{3}$ diffraction pattern. [S0163-1829(96)02720-8]

I. INTRODUCTION

Silicon carbide is an attractive material for electronic device fabrication, particularly for high-temperature and high-voltage applications.[1–4] This and recent developments in growth methods[1–4] to produce high-quality SiC material has made the surface properties of SiC a topic of current interest. Knowledge about the structure and composition of SiC surfaces and changes induced by processing are of fundamental interest, but are also important for device fabrication. Many polytypes of SiC exist,[5] different only in the stacking sequence of the hexagonal bilayers of alternating silicon and carbon atoms. Among these the 3*C* and 6*H* polytypes have been most intensively studied.[6–16]

The present investigation was carried out on Si terminated 6*H*-SiC(0001) surfaces. Previous low-energy electron-diffraction (LEED) studies[8–10,15] have shown that *ex situ* chemically prepared surfaces produce 1×1 LEED patterns directly after introduction into a vacuum. Upon thermal processing at temperatures of about 900 °C, a $\sqrt{3}\times\sqrt{3}$-*R*30° LEED pattern was found to develop.[6–9,15] Further heating to above 1000 °C produced a $6\sqrt{3}\times6\sqrt{3}$-*R*30° pattern,[6,13] which was interpreted to originate from graphitization of the surface, as a result of gradual Si depletion by desorption. For $\sqrt{3}\times\sqrt{3}$ reconstruction, a structural model composed of a $\frac{1}{3}$ layer of Si or C adatoms in threefold symmetric sites on top of the outermost Si-C bilayer was proposed in a recent scanning tunneling microscopy (STM) investigation.[15] The present high-resolution core-level study concentrates on the reconstructed surfaces, but some results for the unreconstructed 1×1 surface are also presented. In a previous investigation[16] of the 3×2 Si-rich 3*C*-SiC(100) surface, two surface-shifted Si 2*p* components were revealed and interpreted to originate from the two topmost surface layers which were thought to be comprised of Si atoms. In the present investigation, high-resolution spectra of the Si 2*p* and C 1*s* levels show the presence of surface shifted components in both levels. These findings are presented below and discussed in view of earlier results.

II. EXPERIMENT

The experiments were performed on beam line 22 at the MAX synchrotron radiation laboratory. This beam line is equipped with a modified SX-700 monochromator,[17] yielding a highly monochromatic photon beam in the UV and soft-x-ray range. The end station of this beam line, which is built up around a large hemispherical Scienta electron analyzer,[18] operates at a base pressure of about 1×10^{-10} mbar. The electron analyzer accepts a cone of angular width ±8°. Normal emission and an incidence angle of 40° was chosen as the experimental geometry. A total-energy resolution, determined by the operating parameters used, of around 80-meV at 130-eV photon energy and of about 200 meV at 330 eV was selected in the high-resolution studies of the Si 2*p* and C 1*s* core levels reported below. The valence-band spectra presented were collected using an energy resolution of about 0.2 eV.

The samples were *n*-doped SiC crystals grown with the Lely method (Ioffe Institute, St. Petersberg, Russia), as well as crystals grown with the modified Lely method (Cree Research Inc., Durham, NC). Samples with different doping concentrations (N, 1×10^{16}–4×10^{18} cm^{-3}) were studied, mainly in an effort to minimize possible broadening caused by band bending effects. Both on-axis and off-axis cut samples were used, some of which were sublimation etched (Ioffe Institute) in order to remove surface damage resulting from the polishing process. The *ex situ* preparation procedure utilized earlier[15] to obtain well-ordered SiC surfaces was applied and the samples were then immediately load locked

into UHV. The as introduced samples displayed the 1×1 LEED pattern expected from a bulk truncated surface. The $\sqrt{3}\times\sqrt{3}$-$R30°$ and $6\sqrt{3}\times6\sqrt{3}$-$R30°$ reconstructed surfaces were prepared, as reported earlier,[15] by resistive heating to temperatures of 950 °C and 1150 °C, as measured with an IR pyrometer. Five different Si-terminated 6H-SiC samples were investigated, but since essentially identical results were obtained, only results from one sample (an on-axis sample from the Ioffe Institute, with a doping concentration of about 3×10^{18} cm^{-3}) are presented. The well-developed reconstructions, labeled $\sqrt{3}$ and $6\sqrt{3}$ below, were obtained after heating for 2 min at 950 °C and 8 min at 1150 °C, respectively. The cleanliness of the samples was checked by monitoring the core levels of likely contaminants (O, N, and F) and by measurements of the valence-band region. For the as introduced 1×1 surface, a strong oxygen and a weak fluorine signal were observed. A weak fluorine signal remained for the $\sqrt{3}$ surface, but for the $6\sqrt{3}$ surface, no contaminants could be detected. The binding energies specified below are referenced to the Fermi level determined from a Ta foil mounted on the sample holder. The high-resolution core-level spectra were recorded with the sample holder cooled to a temperature of about 100 K, in order to minimize broadening effects.

III. RESULTS AND DISCUSSION

Characteristics of the three different surface structures are presented in Sec. III A and some aspects concerning surface graphitization are discussed in Sec. III B. Results obtained when applying a curve-fitting procedure to the recorded C 1s and Si 2p core-level spectra are presented in Secs. III C and III D, and in Sec. III E we discuss possible origins of the extracted surface shifted components.

A. Valence band and core levels

Valence-band spectra recorded from the unreconstructed and reconstructed surfaces, using a photon energy of 130 eV, are shown in Fig. 1. The spectrum from the 1×1 surface is seen to be dominated by contribution from O 2p and O 2s derived states located at energies of about 7 and 25 eV, respectively. The spectra recorded from the two reconstructed surfaces are seen to be distinctly different. They exhibit several sharp and strong features between 0 and 10 eV and some broader and weaker features at larger energies. No oxygen related structures could be detected on these surfaces. Calculated results[19–21] show that the valence-band density of states of SiC can be divided into two subbands. A higher-lying subband composed of hybridized-C 2p and Si $3s+3p$ states and a lower-lying subband dominated by contribution from C 2s electrons. A detailed comparison between valence-band spectra recorded at different photon energies and calculated partial densities of states is reported separately.[21] Here, the recorded valence-band spectra are merely shown as representative fingerprints of the three different surfaces investigated. An important thing to notice is that the $\sqrt{3}$ spectrum show no states at the Fermi level, while states close to the Fermi level are visible in the $6\sqrt{3}$ spectrum.

Spectra recorded of the O 1s region for the three surface structures, using a photon energy of 600 eV are shown in Fig. 2. A strong O 1s signal is observed on the 1×1 surface, while no oxygen signal can be detected on the two reconstructed surfaces. It has been suggested, in recent investigations,[9,10] that the 1×1 surface, prepared *ex situ* and immediately transferred into UHV, include oxygen atoms bound on top of the outermost silicon atoms. For the purpose of estimating if one layer of oxygen atoms can explain the relative strength of the oxygen signal, the core levels of interest were measured using a photon energy of 750 eV. The relative strength of the O 1s signal was found to be 0.63 of the C 1s signal and 0.32 of the Si 2p signal, after dividing the measured intensities with the calculated cross sections.[22] Using a simple layer attenuation model[23] and the approxima-

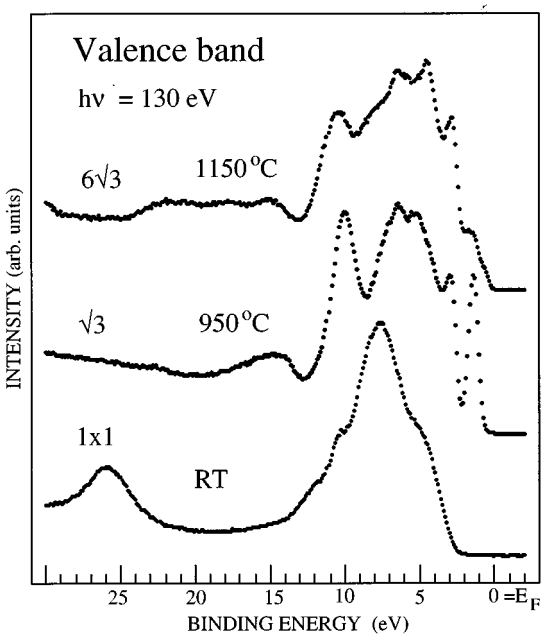

FIG. 1. Valence-band spectra of 6H-SiC(0001), recorded using a photon energy of 130 eV from the unreconstructed 1×1, the $\sqrt{3}$, and the $6\sqrt{3}$ reconstructed surface.

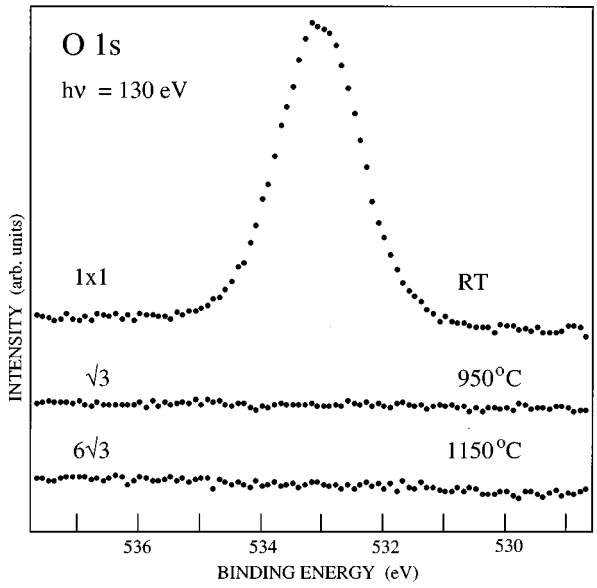

FIG. 2. Spectra recorded of the O 1s region for the three different surface structures, using a photon energy of 600 eV.

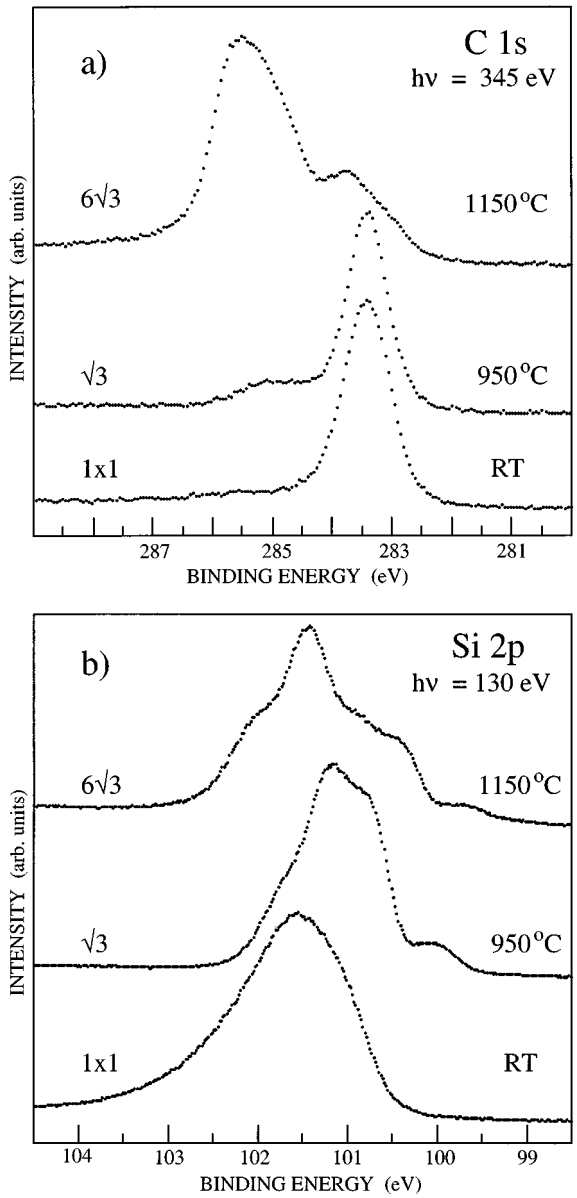

FIG. 3. (a) C 1*s* and (b) Si 2*p* spectra from the unreconstructed 1×1, the $\sqrt{3}$ and the $6\sqrt{3}$ reconstructed 6*H*-SiC(0001) surface.

tion that the oxygen atoms are located 2.5 Å above the Si surface atoms, values of 5.1 and 9.0 Å are obtained for the mean free path at kinetic energies of 450 and 650 eV (which correspond to the kinetic energy of C 1*s* and Si 2*p* electrons, respectively). These values appear reasonable,[24–26] indicating that one layer of oxygen adatoms on a bulk terminated SiC(0001) surface may explain the relative strength observed for the O 1*s* signal on the 1×1 surface.

C 1*s* spectra recorded for the three surfaces, using a photon energy of 345 eV, are shown in Fig. 3(a). The 1×1 spectrum appears to contain only one component, located at a binding energy of 283.4 eV. In the $\sqrt{3}$ spectrum, an additional weaker component is clearly visible at larger binding energy, around 285 eV. The $6\sqrt{3}$ spectrum is dominated by a structure located between 285–286 eV, which has a width and shape that suggest that it contains more than one component. The original lower-lying structure (located around 283.4 eV) is seen to be considerably weaker in this spectrum and to have a shape that suggests that it also contains more than one component. It deserves to be pointed out that this spectrum was recorded on the well-developed $6\sqrt{3}$ reconstruction. A gradual transformation between the $\sqrt{3}$ and $6\sqrt{3}$ reconstructions was observed when heating at temperatures above 950 °C, as discussed further below.

Si 2*p* spectra recorded from the three surfaces, using a photon energy of 130 eV, are shown in Fig. 3(b). The 1×1 spectrum consists of one broad structure, which, when compared to earlier results on Si surfaces,[25,26] must contain more than one spin split Si 2*p* component. That this is the case was clearly revealed by spectra recorded using lower photon energies, i.e., more bulk sensitive spectra, in which the shoulder on the low-binding-energy side in the 130-eV spectrum actually was the dominating feature. If the 1×1 spectrum is assumed to contain only two components, a shift of ca. +0.5 eV is obtained[27] between the low-binding-energy bulk peak and the shifted oxygen related component. An earlier investigation[28] of oxygen adsorption on 3*C*-SiC(001) surfaces showed different oxide features to appear on the high-binding-energy side in the Si 2*p* spectrum. These satellite structures were found to exhibit shifts between about 1 and 3 eV and were compared to the formal oxidation states, +1 to +4, previously revealed on pure Si surfaces.[29] We could not find clear evidence of oxygen related features with such large shifts in the spectra recorded on the as introduced 1×1 surfaces. However, after heating at temperatures between 550–800 °C, an oxide related shoulder appeared in the spectrum at a binding energy of about 2 eV larger than the bulk peak. This observation supports the earlier suggestion[9,10] of adsorbed oxygen atoms on the as introduced surface and rearrangement and oxide formation upon annealing.[28]

For the reconstructed surfaces, the Si 2*p* spectrum is distinctly different. In the $\sqrt{3}$ spectrum, a shoulder is observed on the low-binding-energy side and the shape of the dominating structure indicates that it contains at least two spin split components. In the $6\sqrt{3}$ spectrum, the shoulder on the low-binding-energy side is seen to have shifted to lower binding energy and the main structure is seen to be dominated by a Si 2*p* component located at a somewhat larger binding energy than the components present in the $\sqrt{3}$ spectrum. It should be noted that the Si 2*p*, and also the C 1*s* spectra, were recorded using photon energies giving a high surface sensitivity. The minimum in the electron mean-free-path curve[24–26] is expected to occur at electron kinetic energies in the range 30–50 eV. Minimum mean-free-path values of 3.6 and 3.9 Å have been reported for Si.[25,26] An important message conveyed by these surface sensitive core-level spectra is that both Si and C atoms are present in the outermost layers on all three surfaces, i.e., also for the $6\sqrt{3}$ reconstruction. In addition, the spectra show that the $6\sqrt{3}$ reconstruction is not a result of pure graphitization that has been suggested earlier.[6,13]

B. Surface graphitization

It was recently reported[9] that annealing of the SiC(0001) surface at a temperature above 1000 K gives rise to a low-energy shoulder in the carbon Auger peak, which was assigned to graphitic carbon. The shoulder was reported to appear more pronounced after extensive heating to 1160 K

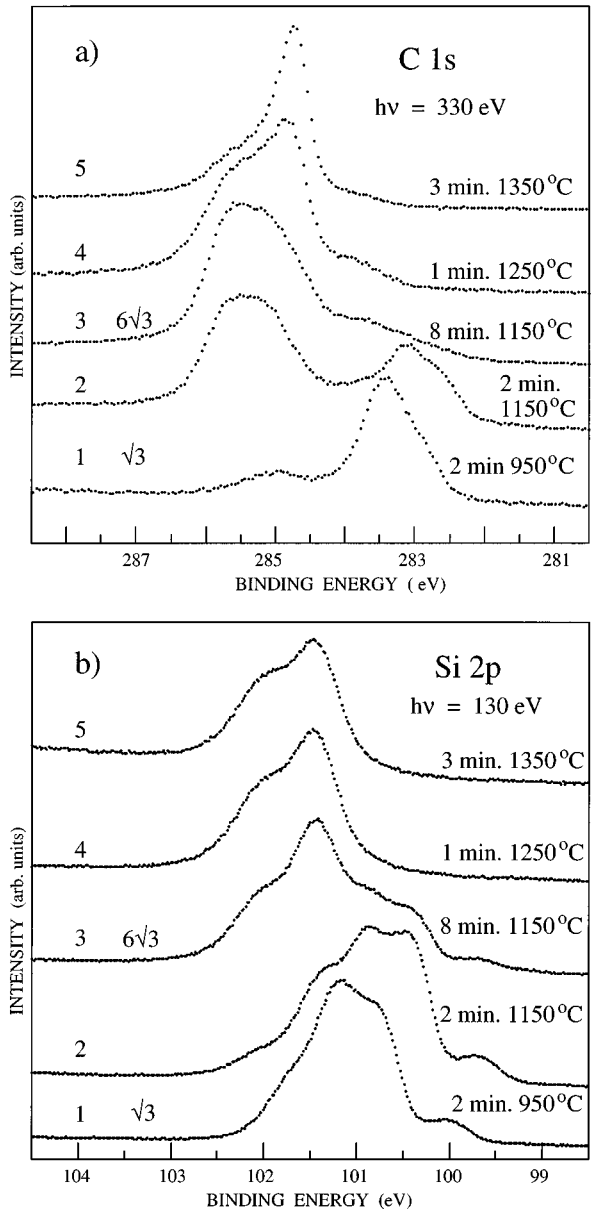

FIG. 4. (a) C 1s spectrum at $h\nu = 330$ eV and (b) Si 2p spectrum at $h\nu = 130$ eV recorded after heating for (1) 2 min at 950 °C (the $\sqrt{3}$ structure), (2) 2 min at 1150 °C, (3) 8 min at 1150 °C (the $6\sqrt{3}$ structure), (4) 1 min at 1250 °C, and (5) 3 min at 1350 °C.

when also the $\sqrt{3}$ reconstruction became visible in the LEED pattern. These findings were in agreement with previous studies[7] and were stated to suggest development of carbon-carbon bonds after Si desorption. In view of these findings, it is worthwhile to consider how the C 1s and Si 2p spectra were observed to change with thermal treatment. High-resolution C 1s and Si 2p spectra recorded after heating at temperatures between 950 and 1350 °C, using a photon energy of 330 eV for C 1s and 130 eV for Si 2p, are shown in Figs. 4(a) and 4(b). Spectra were also recorded at higher energies, up to 500 and 240 eV, respectively, in order to compare the surface sensitive spectra shown in Fig. 4 with more bulk sensitive spectra. The curves labeled 1–5 in Fig. 4 correspond to different heat treatments: (1) 2 min at 950 °C (i.e., the fully developed $\sqrt{3}$ structure), (2) 2 min at 1150 °C, (3) 8 min at 1150 °C (i.e., the well-developed $6\sqrt{3}$ structure as judged from the LEED pattern), (4) 1 min at 1250 °C, and (5) 2 min at 1350 °C. The spectra recorded at the two highest temperatures, labeled 4 and 5, show clear evidence of graphitization. The Si 2p spectrum is seen to consist essentially of one broad spin-orbit split bulk component, located at about 101.4 eV, and shows no surface related components. In the C 1s spectrum, a component interpreted as a graphite C 1s peak appears at a binding energy of 284.7 eV, most pronounced at the highest temperature. The curves labeled 3 correspond to the well-developed $6\sqrt{3}$ reconstruction. In this case, the Si 2p spectrum exhibits surface related features on the low-binding-energy side of the strong bulk component and the C 1s spectrum is dominated by a broad surface related structure located at a slightly larger binding energy than the graphite C 1s peak. This C 1s spectrum shows clearly that the $6\sqrt{3}$ structure is not related to a graphite surface layer, since the shape of the carbon peak is so different from that of the graphite peak, which appears at higher temperatures, as discussed above. There is a large amount of carbon in the surface region, however, and these carbon atoms occupy inequivalent sites, since the broad surface related feature contains more than one component. The curves labeled 2 represent a surface with a mixture of $6\sqrt{3}$ and $\sqrt{3}$ reconstructed areas, since weaker $6\sqrt{3}$ superstructure spots were visible in the LEED pattern, while the $\sqrt{3}$ spots were still fairly strong. The C 1s spectrum exhibits, in this case, two dominant features, which both show additional structure. The high-binding energy feature is interpreted as related to the $6\sqrt{3}$ reconstructed areas and the low-binding-energy feature to the $\sqrt{3}$ reconstructed areas, although the latter is seen to be shifted compared to the dominant structure observed in the C 1s spectrum for the fully developed $\sqrt{3}$ structure (curve 1). The Si 2p spectrum, curve 2, can be interpreted in a similar fashion if the shoulders visible on the high-binding-energy side are assigned to contributions from $6\sqrt{3}$ reconstructed areas (the above assigned bulk peak). The other structures can then be accounted for by shifting the Si 2p peak, obtained for the fully reconstructed $\sqrt{3}$ surface (curve 1), to a smaller binding energy. The Si 2p spectrum for the $\sqrt{3}$ surface, curve 1, is seen to contain at least three spin split components. The main peak in the corresponding C 1s spectrum is seen to contain a shoulder on the low-binding-energy side and a weak broad structure located around 285 eV. It should be noted that the $\sqrt{3}$ reconstruction was found to be stable to prolonged heating. The curves labeled 1 were recorded after heating for 2 min at 950 °C and essentially identical spectra were obtained after heating the surface for 15 min at 950 °C. When increasing the temperature to 1000 °C, or higher, the $6\sqrt{3}$ structure was found to begin to develop.

C. Components in the Si 2p and C 1s spectra

In order to extract the shifts and relative intensities of the different components in the C 1s and Si 2p spectra, for the reconstructed surfaces, a curve fitting procedure[30] was utilized. Some complications were encountered when applying this procedure to SiC. The line-shape parameters are not known for SiC and therefore Lorentzian widths similar to those previously used for Si 2p on silicon[25,26] and C 1s on transition-metal carbides[31] have been used. SiC is a semiconductor with a large band gap, which means that band bending is likely to produce additional broadening.[32] Larger width

parameters, especially for bulk components, could therefore be expected and were also obtained. Samples with different doping concentrations were investigated, but no significant difference in linewidths between low- and high-doped samples was observed. The samples were investigated at a temperature of about 100 K in order to minimize additional broadening effects. For a semiconductor, the asymmetry parameter should be zero, since there are no states at the Fermi level. Recorded valence-band spectra, see Fig. 1, show no states at the Fermi level for the $\sqrt{3}$ reconstruction but, for the $6\sqrt{3}$ structure states, are present close to or at the Fermi level, which may give rise to an asymmetry in the core levels. Several components were needed to fit these core-level spectra, so some constraint on the parameters had to be introduced in the fitting procedure. The approach used[33] was to select one Lorentzian width and asymmetry parameter for all components in a spectrum, but to allow the Gaussian width to vary independently for each component. The Gaussian width does, therefore, correspond not only to the instrumental broadening, but also includes other broadening effects. Spectra were recorded at several photon energies between 315 and 500 eV for the C 1*s* level and between 115 and 240 eV for the Si 2*p* level. A linear background model was applied in most cases, except for spectra recorded at such low kinetic energies that the curvature of the inelastic tail had to be accounted for. In this case, i.e., at photon energies $\leqslant$120 eV for the Si 2*p* level and $\leqslant$320 eV for the C 1*s* level, an exponential background model had to be used. The background is included in all the fits presented below.

The results of applying the curve-fitting procedure to C 1*s* spectra are shown in Figs. 5(a)–5(c). In each figure, the raw data recorded using a photon energy of 330 (surface sensitive) and 500 eV (less surface sensitive) are shown by dots. The curves below the 330-eV spectrum show the components used and the curve through the data points show the result of the fit. The C 1*s* spectrum for the $\sqrt{3}$ structure, Fig. 5(a) shows two surface components besides a bulk component located at 283.4 eV. The surface components, located at 282.8 and 285.0 eV, are directly discernible in the recorded curve. For the well-developed $6\sqrt{3}$ structure, Fig. 5(c), the C 1*s* spectrum is dominated by a broad surface related structure, which contains, at least, two components: a broad and strong component located around 285.3 eV and a weaker and narrower one around 285.7 eV. Since one component is so broad, efforts to use three components were made but were unsuccessful. No consistency in relative intensities with photon energy between the different components could then be obtained. The low-energy structure, most pronounced in the 500-eV spectrum and thus bulk related, contains in this case two components, a strong one located at 283.8 eV and a weaker one located around 283.1 eV. The spectra shown in Fig. 5(b) were recorded on the surface where the $6\sqrt{3}$ structure had started to develop (same as curve 2 in Fig. 4). The high-binding-energy structure is decomposed into two components also in this case and the broad one is seen to be even more dominating than in Fig. 5(c). Two bulk components are obtained in this case, one stronger located at 283.1 eV and a weaker one located around 283.8 eV. A shoulder is clearly visible on the low-binding-energy side in the 330-eV spectrum and yields a surface related component around 282.8 eV. At first glance it appears strange that two bulk components can be observed. Considering that this surface has a mixture of $\sqrt{3}$ and $6\sqrt{3}$ reconstructed areas, this can however be explained by a difference in Fermi-level pinning for the two reconstructions.

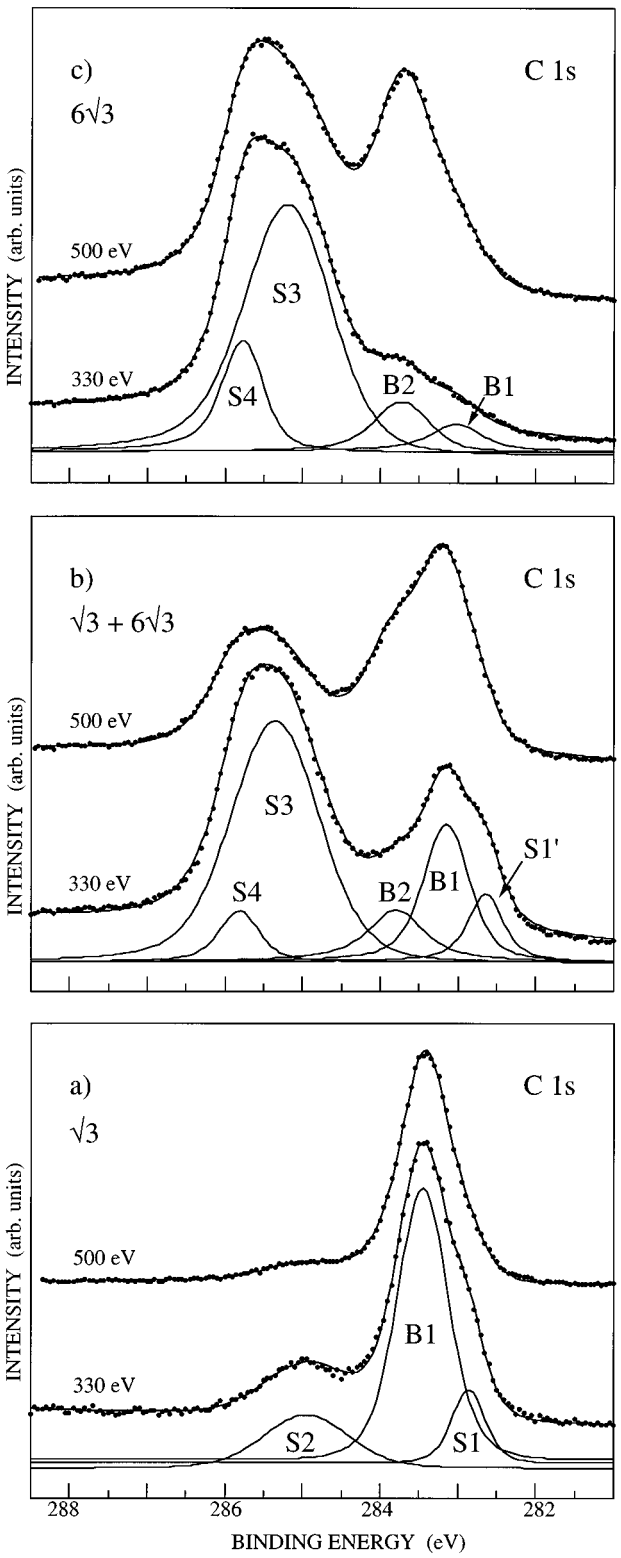

FIG. 5. C 1*s* spectra recorded using two different photon energies are shown by the dots. The solid curves through the data points show the result of the curve fit and the curves underneath the 330-eV spectrum show the components used. Labels (a), (b), and (c) correspond to 1, 2, and 3 in Fig. 4, i.e., to the $\sqrt{3}$, the mixture of $\sqrt{3}$ and $6\sqrt{3}$, and the $6\sqrt{3}$ reconstructed surface.

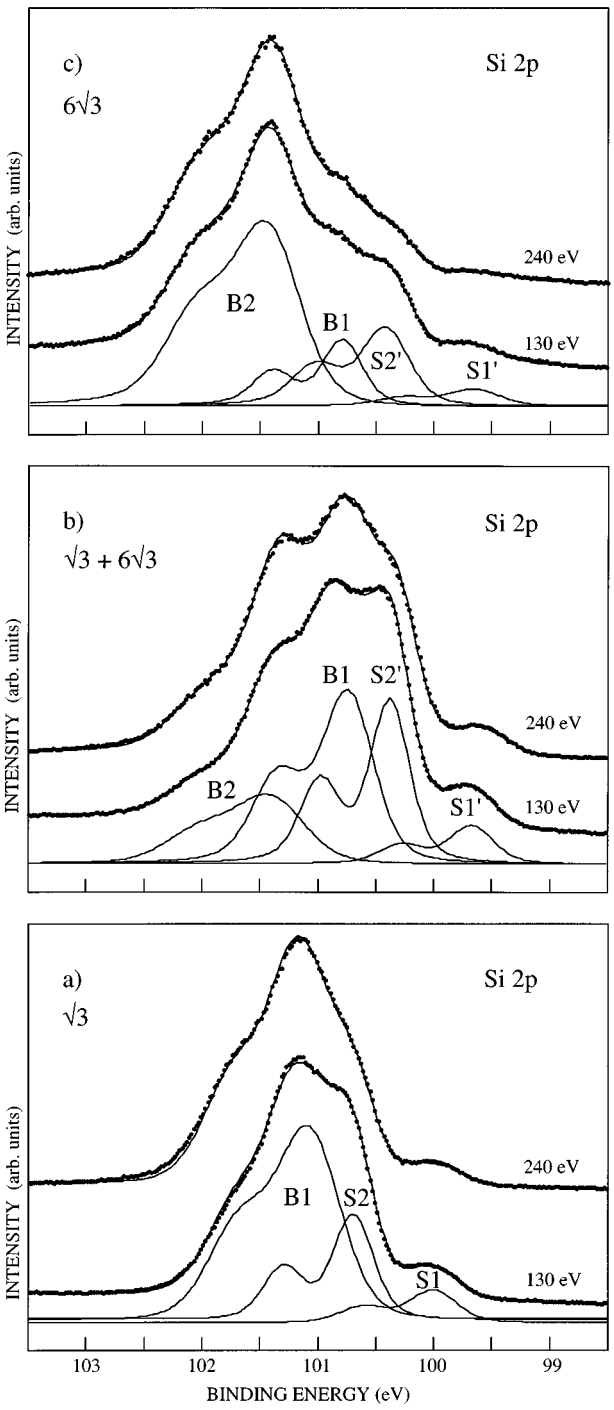

FIG. 6. Si $2p$ spectra recorded using two different photon energies are shown by the dots. The solid curves through the data points show the result of the curve fit and the curves underneath the 130-eV spectrum show the components used. Labels (a), (b), and (c) correspond to 1, 2, and 3 in Fig. 4, i.e., to the $\sqrt{3}$, the mixture of $\sqrt{3}$ and $6\sqrt{3}$, and the $6\sqrt{3}$ reconstructed surface.

Fits of the Si $2p$ spectra are shown in Figs 6(a)–6(c). In each figure, the raw data recorded using a photon energy of 130 (surface sensitive) and 240 eV (less surface sensitive) are shown by dots. The curves below the 130-eV spectrum show the components used and the curve through the data points show the result of the fit. For the $\sqrt{3}$ reconstructed surface, Fig. 6(a), two surface components are obtained besides the bulk component located at 101.1 eV. The bulk component is seen to be considerably broader than the surface shifted components. For the fully developed $6\sqrt{3}$ reconstruction, an even broader bulk component is extracted, located at 101.4 eV. Three additional components are resolved in this case, two of which are clearly surface related, since their contribution is considerably weaker in the 240-eV spectrum. The third of these components, the one located at about 100.7 eV, is not much attenuated in the 240-eV spectrum and is not a surface component. The origin of this feature is obvious when looking at the fit in Fig. 6(b), i.e., for the surface containing a mixture of $\sqrt{3}$ and the $6\sqrt{3}$ reconstructed areas. Two bulk components are resolved, located at energies of 100.7 and 101.4 eV respectively, and interpreted to originate from the $\sqrt{3}$ and $6\sqrt{3}$ reconstructed areas. The two other components, located at 100.3 and 99.7 eV, are clearly surface related.

The picture thus appears very similar when looking at the C $1s$ and Si $2p$ spectra. The bulk component for the $\sqrt{3}$ reconstruction is shifted about 0.4–0.5 eV towards smaller binding energy when the $6\sqrt{3}$ reconstruction begins to develop and a new bulk component shifted about 0.3–0.4 eV towards larger binding energy appears. For the well-developed $6\sqrt{3}$ structure the high-binding energy bulk component is found to be the dominating one. Surface related components are unambiguously identified in the C $1s$ and Si $2p$ spectra for both the $\sqrt{3}$ and $6\sqrt{3}$ surfaces. The widths obtained for the different components deserve a comment, particularly since the Si $2p$ bulk components are found to be so different for the $\sqrt{3}$ and $6\sqrt{3}$ surfaces. That a bulk component is broader than a surface component can for SiC most likely be attributed to band bending effects. This may also be a reason why the bulk Si $2p$ component on the $6\sqrt{3}$ surface is considerably broader than on the $\sqrt{3}$ surface, since our results indicate that the Fermi-level pinning is different for these surfaces. The additional broadening may, however, also originate from compositional variations with depth from the surface or from the presence of different defects. These high-resolution core levels show, however, unambiguously that surface shifted C $1s$ and Si $2p$ components do exist both on the $\sqrt{3}$ and the $6\sqrt{3}$ reconstructed surface. The extracted core-level shifts and the Gaussian widths obtained in the fits are summarized in Table I for the two reconstructed surfaces.

D. The C 1*s* graphite peak

For the purpose of elucidating in somewhat greater detail the development of the graphitic C $1s$ component, fits of spectra recorded after heating at 1250 °C and 1350 °C are shown in Fig. 7. These are seen to contain a bulk component, located around 283.8 eV, and two surface components. The one located at 284.7 eV becomes strong and fairly narrow after heating at the highest temperature and is interpreted to be the graphitic C $1s$ peak. The broader surface component, located at about 0.5-eV-larger binding energy, indicates the presence of surface carbon in a different form than graphite. The Si $2p$ spectrum is dominated by one broad bulk component in these cases, as illustrated in Fig. 8. However, a weak contribution of additional components on the low-binding-energy side is revealed by the fits. For these two surfaces, the LEED pattern showed the $6\sqrt{3}$ structure spots, but also a significantly larger background contribution, largest at the

TABLE I. Binding energy (BE) and surface core-level shift (SCLS) in eV for components resolved for the $\sqrt{3}$ and $6\sqrt{3}$ reconstructions. The Gaussian width (GW) in eV used for each component is also specified. The binding energy referenced to the Fermi level of a Ta foil were determined with an accuracy of ± 0.1 eV. The surface core-level shifts are given relative to the $B1$ component. In each case, the mean value specified was obtained from at least six independent determinations and the maximum deviation is given in parentheses.

	C 1*s* level		Si 2*p* level	
$\sqrt{3}$ reconstruction	BE/SCLS	GW	BE/SCLS	GW
$B1$ bulk comp.	283.4	0.60	101.1	0.55
$S1$ surf. comp.	-0.61 (± 0.05)	0.32	-1.10 (± 0.04)	0.40
$S2$ surf. comp.	$+1.46$ (± 0.09)	1.35	-0.41 (± 0.04)	0.33
	C1*s*level		Si2*p*level	
$6\sqrt{3}$ reconstruction	BE/SCLS	GW	BE/SCLS	GW
$B2$ bulk comp.	283.8	0.64	101.4	0.57
$B1$ bulk comp.	283.1	0.64	100.7	0.31
$B2$-$B1$ separation	$+0.66$ (± 0.06)		$+0.65$ (± 0.06)	
$S1'$ surf. comp.			-1.16 (± 0.06)	0.43
$S2'$ surf. comp.			-0.39 (± 0.06)	0.39
$S3$ surf. comp.	$+2.11$ (± 011)	1.20		
$S4$ surf. comp.	$+2.67$ (± 0.15)	0.51		

highest temperature. The most distinct $6\sqrt{3}$ pattern was obtained for the surface we have labeled ''well-developed $6\sqrt{3}$,'' which was prepared by heating at 1150 °C for 8 min.

E. Origin of the surface shifted components

Surface shifted components in both the C 1*s* and Si 2*p* core levels were unambiguously identified in the high-resolution spectra presented above for the reconstructed surfaces. Ideally one would like to assign these shifted components with specific sites for the atoms. In a previous investigation[16] of the 3×2 Si-rich $3C$-SiC(100) surface, two surface shifted Si 2*p* components having shifts of -0.48 and -1.41 eV, were revealed. These components were interpreted to originate from the two outermost layers, a buckled topmost Si layer and a Si layer underneath. The component exhibiting the largest shift was assigned to up atoms in the buckled topmost layer and the component showing the smaller shift was interpreted to originate from the other atoms in the topmost layer, plus the atoms in underlying layer. The 3×2 Si-rich $3C$-SiC(100) surface was prepared by exposing the sample to a flux of Si, from an evaporation source, during heating. In our case, the reconstructed surfaces were prepared by *in situ* heating of 6*H*-SiC samples, which after load locking into UHV showed 1×1 LEED patterns. For the $\sqrt{3}$ and $6\sqrt{3}$ reconstructions, we can rule out the possibility that the two topmost layers are comprised solely of Si atoms, since prominent surface C 1*s* components are observed in both cases. For the $6\sqrt{3}$ structure, our results show that the surface region contains a considerably larger amount of carbon than silicon compared to the $\sqrt{3}$ structure, since the relative strength of the surface C 1*s* (Si 2*p*) components are larger (smaller) for the $6\sqrt{3}$ reconstruction than for the $\sqrt{3}$ reconstruction. Moreover, the drastic changes observed in both the C 1*s* and Si 2*p* spectrum show that the structural change from the $\sqrt{3}$ to the $6\sqrt{3}$ is accompanied by quite large changes in the chemical composition in the surface region. For the $6\sqrt{3}$ structure, an interesting point is if one surface layer of carbon can give rise to such strong surface components. An estimate of the largest surface to bulk intensity ratio to be expected using the layer attenuation model, a bilayer separation of 2.52 Å, and the minimum mean-free-path values previously reported,[24–26] yield a ratio of $\leqslant 1.3$. A considerably larger intensity ratio is extracted from the 330-eV spectrum, as shown in Fig. 5(c), which suggests that more than one layer is affected in this reconstruction. For the $\sqrt{3}$ structure, on the other hand, the relative strength of the extracted surface components in both the C 1*s* and Si 2*p* spectrum is small enough for each of them to be interpreted as contribution from one surface layer or less.

For the $\sqrt{3}$ reconstruction, a structural model composed of $\frac{1}{3}$ layer of Si or C adatoms in threefold symmetric sites on top of the outermost Si-C bilayer was proposed in a recent STM investigation.[15] This model, however, cannot explain the occurrence of two surface shifted components in both the Si 2*p* and C 1*s* level, as observed for the $\sqrt{3}$ surface. If the adatoms are assumed to be Si atoms, one can account for the two shifted components observed in the Si 2*p*. The $S1$ component can be assigned to the Si adatoms and the $S2$ component to the Si atoms in the topmost bilayer. We rule out the possibility that Si atoms in the bilayer underneath the topmost bilayer contributes to $S2$, since a considerably larger surface to bulk intensity ratio would then be expected. The problem encountered is how to interpret the two shifted components appearing in the C 1*s* spectrum. One component can be accounted for, the $S1$ component, which can be interpreted to originate from carbon atoms in the topmost bilayer. The $S2$ component, appearing at a larger binding energy than the bulk peak, is however difficult to find an explanation for. The presence of defect areas may be envisioned, but it appears unlikely since the recent STM results[15] indicate that

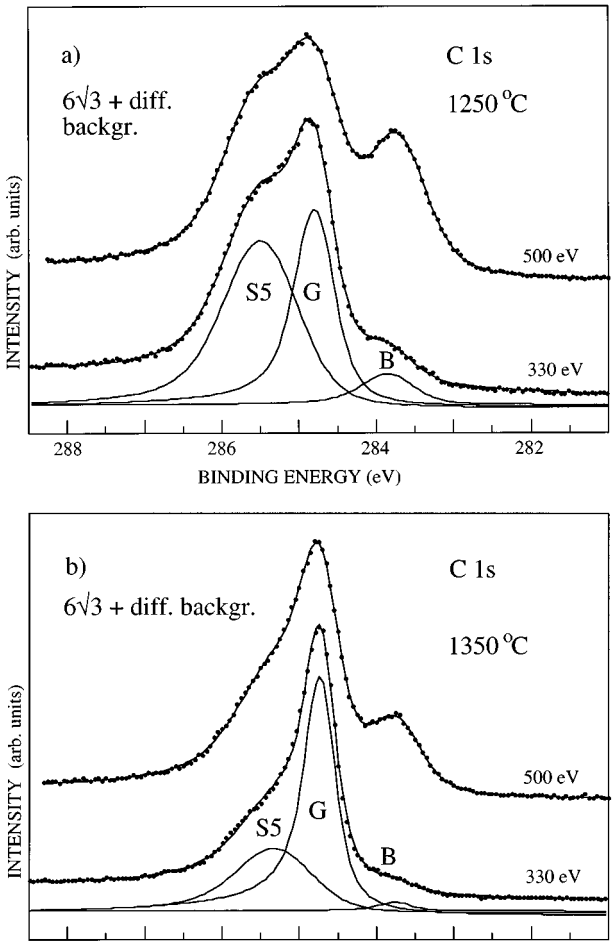

FIG. 7. C 1s spectra recorded using two different photon energies are shown by the dots. The solid curves through the data points show the fitted curves and the curves underneath the 330-eV spectrum the components used. Labels (a) and (b) correspond to 4 and 5 in Fig. 4, i.e., to heating 1 min at 1250 °C and 3 min at 1350 °C, respectively. The LEED pattern showed the $6\sqrt{3}$ spots, but also a large diffuse background contribution in these cases.

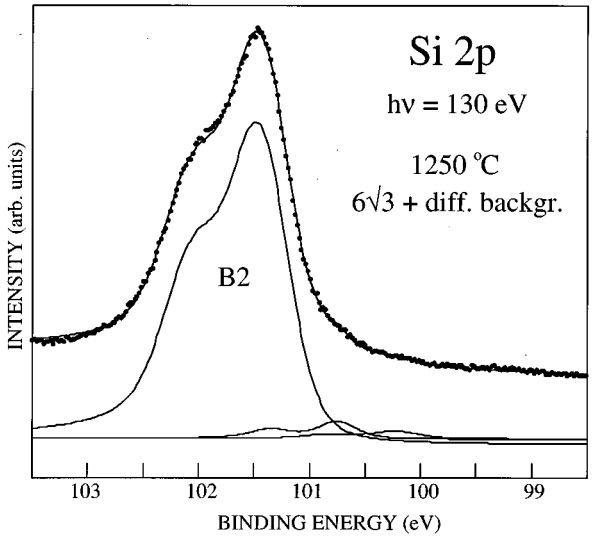

FIG. 8. Si $2p$ spectrum recorded using a photon energy of 130 eV after heating 1 min at 1250 °C, i.e., corresponding to 4 in Fig. 4. The LEED pattern showed the $6\sqrt{3}$ spots, but also a large diffuse background contribution.

the concentration of defects is too small to account for a surface component of this magnitude. A similar difficulty of assigning the four surface shifted components is encountered if the adatoms instead are assumed to be C atoms. If the $S2$ component in the C $1s$ spectrum is assigned to the C adatoms and the $S1$ component to the C atoms in the topmost bilayer, the problem then concerns the two shifted components in the Si $2p$ spectrum. One of these can then be assigned to the Si atoms in the topmost bilayer, but the occurrence of a second component with a distinctly different relative strength is difficult to explain. One possibility to account for these shifted levels would be to assume regions with different terminations to exist on the surface, i.e., the presence of C and Si terminated areas. This possibility seems unlikely, however, in view of the recent STM results.[15] Adatoms of Si, or C, in threefold symmetric sites on top of the outermost Si-C bilayer are moreover not consistent with our observation that the valence-band spectrum for the $\sqrt{3}$ surface show no states at the Fermi level. These adatoms should produce a metallic surface,[34] which is not observed experimentally.

The above arguments concerning the existence of two surface shifted components in both Si $2p$ and C $1s$ level for the $\sqrt{3}$ reconstruction also rule out an interpretation in terms of a trimer arrangement of C, or Si atoms on top of the outermost Si-C bilayer.[15] From cluster calculations,[35,36] hydrogenated triangles of C atoms saturating the surface silicon dangling bonds in the outermost Si-C bilayer has been proposed as the most favorable model for the $\sqrt{3}$ reconstruction. This model cannot, however, explain our experimental results.

Other possible arrangements have, therefore, to be considered. One option is to assume that the topmost bilayer is modified in the $\sqrt{3}$ reconstruction, such that $\frac{2}{3}$ of the Si atoms are desorbed so the only Si atoms remaining are the adatoms on top of an arrangement of C atoms. The second bilayer could be assumed to be affected by these rearrangements to such an extent that also these atoms should give rise to surface shifted components. This would explain the observation of two shifted components in both levels and also the appearance of a surface C $1s$ component shifted to larger binding energy. The observed components could then be assigned as follows. The $S1$ component in the Si $2p$ spectrum to the Si adatoms and the $S2$ component to Si atoms in the second bilayer. The $S2$ component in the C $1s$ spectrum to C atoms in a modified (''carburized'') topmost bilayer, and the $S1$ component to C atoms in the second bilayer. This would also be consistent with the extracted relative intensities of the different components. In the Si $2p$ spectrum, the $S1$ component is considerably smaller than the $S2$ component, while in the C $1s$ spectrum, the magnitude of the broad $S2$ and the narrower $S1$ component are fairly similar. At present, we can only speculate about various possible arrangements of C atoms in such a modified layer, since no theoretical results are, as far as we know, available to predict the core-level shift resulting from a certain change in carbon bonding configuration on SiC. One could, for example, consider a trimer arrangement of C atoms above the second bilayer and under-

neath the adatoms, since this would not be in conflict with the previous STM observations.[15] Trimers would give rise to substantial changes in the carbon bonding configuration and could be assumed to produce a more graphitelike C 1*s* component, like the *S*2 component observed. In a trimer model it is, however, difficult to envision how the strain induced in the bonds are accommodated. Therefore, a more complex arrangement of C atoms in a layer underneath Si adatoms seems to be required to explain the shifted levels observed. At present, we cannot propose a specific arrangement, but hope that future theoretical efforts concerning core-level shifts in SiC may provide new insight concerning the structure of the $\sqrt{3}$ reconstruction. What we can do is to list the experimental observations that such a structural model for the $\sqrt{3}$ surface should account for in order to be consistent with our photoemission results. It should account for two surface Si 2*p* levels shifted to smaller binding energies and for a considerably weaker relative strength for the component exhibiting the largest shift. It should account for two surface C 1*s* components of comparable relative strength, one exhibiting a negative shift and one a positive shift. Finally, it should account for a semiconducting surface.

One puzzling observation is made concerning the core-level intensities when comparing the $\sqrt{3}$ and the $6\sqrt{3}$ structure. In the Si 2*p* spectrum, shown in Fig. 6, the surface-to-bulk intensity ratios ($S1/B1$ and $S2/B1$) are seen to increase in going from the $\sqrt{3}$ to the $6\sqrt{3}$ reconstruction. These two surface shifted Si 2*p* components were above interpreted to be related solely to the $\sqrt{3}$ reconstruction. The LEED pattern and also STM images[37] suggest that the $6\sqrt{3}$ reconstruction begins to develop in certain areas on the surface, while the rest remains $\sqrt{3}$ reconstructed when increasing the heating temperature from 950 °C to 1150 °C. If the changes induced were restricted to the two outermost bilayers, one would expect the surface-to-bulk intensity ratio related to the $\sqrt{3}$ structure to remain constant, i.e., contrary to our experimental observation. This suggests that changes in deeper lying bilayers accompany the structural transformation, since the bulk component related to the $\sqrt{3}$ structure decrease in relative intensity when the areas of $6\sqrt{3}$ reconstruction increase. The $6\sqrt{3}$ structure has been suggested to form upon Si depletion by desorption and Si atoms must then diffuse to the surface before desorption when more than one bilayer is affected. One way to explain the strange behavior of the bulk component related to the $\sqrt{3}$ structure is to assume that bulk diffusion creates a concentration profile fairly deep into the solid so that the bulk component for the $6\sqrt{3}$ structure actually develops underneath the areas showing the $\sqrt{3}$ reconstruction on the surface. The bulk component related to the $\sqrt{3}$ structure does not disappear until clear evidence of graphitization of the surface is obtained, as seen in Figs. 7(a) and 8. For the $\sqrt{3}$ areas, it appears as if a certain Si concentration gradient is maintained in the outermost layers by diffusion from deeper layers.

IV. SUMMARY

For the as introduced 1×1 surface, strong oxygen related features are identified in the valence-band spectra. One layer of oxygen atoms on top of a bulk terminated surface is found to be a reasonable estimate from the relative strength obtained for the O 1*s* signal. Upon heating, the oxygen is found to disappear before the $\sqrt{3}$ reconstruction develops. Valence-band spectra recorded from the $\sqrt{3}$ and $6\sqrt{3}$ reconstructions show distinct differences, but no oxygen related features.

The high-resolution core-level results for the $\sqrt{3}$ reconstruction show unambiguously the presence of two surface shifted levels in both the Si 2*p* and C 1*s* levels. This cannot be explained using a model of Si or C adatoms on top of a bulk terminated Si-C bilayer. Instead, we propose a model in which the topmost bilayer is modified, such that only $\frac{1}{3}$ of the Si atoms remain as adatoms on top of a modified arrangement of C atoms. The adatoms, the modified carbon layer, and the bilayer underneath are proposed to give rise to the surface shifted components observed.

For the well-developed $6\sqrt{3}$ reconstruction, the surface region is found to contain a large amount of carbon, as revealed by strong surface related features in the C 1*s* spectrum. This carbon is found not to be graphitic, since two surface related components appear with binding energies different from the graphitic C 1*s* peak observed after heating at higher temperatures. The changes observed in the core levels when the surface transforms from the $\sqrt{3}$ to the $6\sqrt{3}$ structure suggest that compositional changes are induced several layers deep into the crystal and that the Fermi-level pinning is different on $\sqrt{3}$ and $6\sqrt{3}$ reconstructed areas. Clear evidence of graphitization, i.e., the appearance of a graphitic C 1*s* peak, is revealed only after heating to a higher temperature than that required for observing a well-developed $6\sqrt{3}$ LEED pattern.

ACKNOWLEDGMENTS

Financial support from the Swedish Natural Research Council and the Swedish Research Council for Engineering Sciences (F.O. and P.M.) is gratefully acknowledged.

[1] G. Pensl and R. Helbig, in *Festkörperprobleme: Advances in Solid State Physics*, edited by U. Rössler (Vieweg, Braunschweig, 1990), Vol. 30, p. 133.

[2] O. Kordina, J. P. Bergman, A. Henry, E. Janzén, S. Savage, J. André, L. P. Ramberg, U. Lindefelt, W. Hermansson, and K. Bergman, Appl. Phys. Lett. **67**, 1561 (1995).

[3] R. F. Davis, J. W. Palmour, and J. A. Edmond, *International Electron Device Meeting Technical Digest* (IEEE, New York, 1990), Vol. 90, p. 785.

[4] M. Bhatnagar and B. J. Baliga, IEEE Trans. Electron Devices **40**, 645 (1993).

[5] R. Verma and P. Krishna, *Polymorphism and Polytypism in Crystals* (Wiley, New York, 1966).

[6] A. J. van Bommel, J. E. Crombeen, and A. van Tooren, Surf. Sci. **48**, 463 (1975).

[7] R. Kaplan, Surf. Sci. **215**, 111 (1989).

[8] S. Nakanishi, H. Tokutaka, K. Nishimori, S. Kishida, and N. Ishihara, Appl. Surf. Sci. **41/42**, 44 (1989).

[9] U. Starke, Ch. Bram, P.-R. Steiner, W. Hartner, L. Hammer, K. Heinz, and K. Müller, Appl. Surf. Sci. **89**, 175 (1995).
[10] J. Schardt, Ch. Bram, S. Müller, U. Starke, K. Heinz, and K. Müller, Surf. Sci. **337**, 232 (1995).
[11] L. Muehlhoff, W. J. Choyke, M. J. Bozack, and J. T. Yates, Jr., J. Appl. Phys. **60**, 2842 (1986).
[12] M. A. Kulakov, P. Heuell, V. F. Tsvetkov, and B. Bullemer, Surf. Sci. **315**, 248 (1994).
[13] C. S. Chang, I. S. T. Tsong, Y. C. Wang, and R. F. Davis, Surf. Sci. **256**, 354 (1991).
[14] S. Tyc, J. Phys. (France) I **4**, 617 (1994).
[15] F. Owman and P. Mårtensson, Surf. Sci. **330**, L639 (1995).
[16] M. L. Shek, K. E. Miyano, Q.-Y. Dong, T. A. Calcott, and D. L. Ederer, J. Vac. Sci. Technol. A **12**, 1079 (1994).
[17] R. Nyholm, S. Svensson, J. Nordgren, and S. A. Flodström, Nucl. Instrum. Methods Phys. Res. Sect. A **246**, 267 (1986).
[18] J. N. Andersen, O. Björnholm, A. Sandell, R. Nyholm, J. Forsell, L. Thånell, A. Nilsson, and N. Mårtensson, Synch. Radiat. News **4**, 15 (1991).
[19] Yuan Li and P. J. Lin-Chung, Phys. Rev. B **36**, 1130 (1987).
[20] C. H. Park, Byoung-Ho Cheong, Keun-Ho Lee, and K. J. Chang, Phys. Rev. B **49**, 4485 (1994).
[21] L. I. Johansson, F. Owman, P. Mårtensson, C. Persson, and U. Lindefeldt, following paper, Phys. Rev. B **53**, 13 798 (1996).
[22] J. J. Yeh and I. Lindau, At. Data Nucl. Data Tables **32**, 1 (1985).
[23] Using the layer attenuation model, the intensity ratio between a surface layer and the bulk can, when the same concentration of atoms is assumed in each layer, be expressed as $R=e^{d/\lambda}-1$, where d is the interlayer distance (bilayer distance of 2.52 Å in this case) and λ the electron mean free path. Since λ depends on the electron kinetic energy, the O 1s/C 1s and C 1s/Si 2p ratios determined can be used to estimate λ at those two different kinetic energies.
[24] M. P. Seah and W. A. Dench, Surf. Interface Anal. **1**, 2 (1979).
[25] G. K. Wertheim, D. M. Riffe, J. E. Rowe, and P. H. Citrin, Phys. Rev. Lett. **67**, 120 (1991).
[26] E. Landemark, C. J. Carlsson, Y.-C. Chao, and R. I. G. Uhrberg, Phys. Rev. Lett. **69**, 1588 (1992).
[27] The shift was extracted using the curve-fitting procedure described in Ref. 30 and in Sec. III C.
[28] V. M. Bermudez, J. Appl. Phys. **66**, 6084 (1989).
[29] F. J. Himpsel, F. R. McFeely, A. Taleb-Ibramhimi, J. A. Yarmoff, and G. Hollinger, Phys. Rev. B **38**, 6084 (1988).
[30] P. H. Mahowald, D. J. Friedman, G. P. Carey, K. A. Bertness, and J. J. Yeah, J. Vac. Sci. Technol. A **5**, 2982 (1987).
[31] See references given in L. I. Johansson, Surf. Sci. Rep. **21**, 5 178 (1995).
[32] That the bilayers of the 6H polytype are nonequivalent is probably of lesser importance.
[33] Fit procedures selecting values for the Gaussian widths and asymmetry parameter and allowing the Lorentzian width to vary were also tried, but did not yield better fits. Results are presented when Lorentzian widths of 0.15 and 0.30 eV for the Si 2p and C 1s levels were selected. A branching ratio of 0.5 and a spin-orbit split of 0.602 eV was used for the Si 2p doublet. Asymmetry parameter values of 0, 0.01, and 0.03 were found to produce best fits to the spectra recorded from, respectively, the $\sqrt{3}$, the mixed $\sqrt{3}$, and $6\sqrt{3}$, and the $6\sqrt{3}$ reconstructed surface.
[34] J. E. Northrup, Phys. Rev. Lett. **57**, 154 (1986).
[35] P. Badziag, Surf. Sci. **337**, 1 (1995).
[36] P. Badziag, Surf. Sci. (to be published).
[37] F. Owman and P. Mårtensson, J. Vac. Sci. Technol. B **14**, 933 (1996).